

UDC 621.125

CONTACT DEFORMATION OF THE PIPELINE SEALING UNIT

¹ **Andrii O. Kostikov**kostikov@ipmach.kharkov.ua

ORCID: 0000-0001-6076-1942

² **Serhii A. Palkov**sergpalkov@gmail.com

ORCID: 0000-0002-2215-0689

¹ A. Pidhornyi Institute
of Mechanical Engineering
Problems of NASU,
2/10, Pozharskyi St.,
Kharkiv, 61046, Ukraine

² JSC "Turboatom"
199, Moskovskiy Ave.,
Kharkiv, 61037, Ukraine

The features of the turbine steam line sealing unit stress-strain state are examined on the basis of the usage of a three-dimensional design model of the construction and contacting surfaces. The considered unit consists of the pipeline, a crimp casing consisting of two halves with an outlet in one of them, and a gasket. A mathematical model that takes into account the mechanical loads caused both by the internal steam pressure on the steam line wall and by the casing fasteners tightening has been formed. This model also includes contact interaction in the sealing unit on the contact surface of the pipeline, the upper and lower halves of the casing. This contact problem solving method, based on the application of the finite element method, is proposed. The finite element model is based on twenty-unit three-dimensional finite elements with three degrees of freedom at each unit. Eight-unit contact finite elements were used to describe contact and sliding between surfaces. Contact conditions are taken into account with the penalty method usage. The verification of the model and the software that implements the proposed method is carried out by comparing the calculation results and experimental data obtained on the physical model of the pipeline. The physical model was made from a low-modulus material with full geometric similarity and the same ratio of the elastic moduli of materials as in a real object. The stress-strain state of the sealing unit of a real pipeline in a three-dimensional setting was determined and the most stressed zones in the unit, which require increased attention during the design and operation of pipelines and their connections, were identified. The developed approach and software make it possible to determine the contact pressure for the horizontal joint flanges of highly stressed cylinder bodies of powerful steam turbines, which helps to avoid a large number of expensive experimental studies.

Keywords: turbine, pipeline, flange connection, contact problem, stress-strain state, contact.

Introduction

One of the most important and common elements of modern thermal power plants are pipelines of various diameters and configurations, designed for transportation of steam, water, oil, gas, air, fuel oil and other media. Pipelines connect the main units of the power plant and auxiliary equipment. As a result of thermal equipment combining with a system of pipelines, a single construction that performs the main technological process of electricity production is formed.

The reliability and efficiency of a thermal power plant operation is largely determined by the reliable and economical operation of its pipeline system. The pipelines damage may lead to the need to reduce the power of the units or even to their complete stop.

Pipelines in modern thermal power plants represent a complex spatial system that consists of both pipes themselves and means that connect them together [1].

The object of research in this paper is a sealing unit for a branch inset into a steam line that operates under the influence of internal steam pressure.

The purpose of this work is a development of methodology, based on the use of three-dimensional models, for solving a contact problem for a pipeline sealing unit, its verification by comparing the calculation results with experimental data, as well as identification of the most stressed zones in the unit that require increased attention during the pipelines and their connections designing and operation.

The assessment of the stress-strain state (SSS) of the sealing unit for the branch inset into the steam pipeline is a very urgent problem, according to the foresaid.

Formulation of the problem

The problem of the sealing unit SSS determination will be considered in an elastic formulation, without taking into account the influence of temperature stresses and deformations. The pipeline connecting unit under study is shown in Fig. 1. There is also a loading scheme that takes into account:

- internal pressure on the wall of the steam line, which is 7.5 MPa (loads of "A" group);
- tightening of the casing fasteners, which is 6.25 MPa (loads of "B" group);

In addition, the considered problem takes into account the contact interaction in the sealing unit on the contacting surface of the pipeline.

Boundary conditions that simulate the fastening of the sealing unit in the calculated three-dimensional model are constructed proceeding from the limitation of the unit displacement along the vertical axis (Fig. 1).

The physical and mechanical properties of materials (Young's modulus E , Poisson's ratio ν , density ρ) used during the sealing unit manufacture are given in table 1 [2, 3].

Finite element model and additional conditions of the contact problem

The problem of the pipeline sealing unit SSS determination was solved on the basis of a three-dimensional model, which is an assembly of the main pipeline, the upper and lower halves of the casing seal and the seal itself – paronite.

To carry out this calculation on a 1:1 scale in the CAD package Autodesk Inventor [4], a steam line connector geometric model, which was further imported into software package ANSYS based on the finite element method (FEM), was created. As a result, a computational finite element model of the sealing unit was created. By splitting the original model, about 490,000 finite elements were obtained (Fig. 1).

When creating a finite element model, a twenty-unit three-dimensional element with three degrees of freedom at each unit, depicted in Fig. 2, was used [5]. This element has a quadratic representation of displacements and can be used both in regular and irregular grids, which is important when building

computational finite element models for objects of a sufficiently complex geometric structure that were imported from various software systems for designing.

For a more accurate determination of the stress-strain state, the used three-dimensional model includes a symmetrical contact interaction of two halves of the casing, the gasket seal and the main pipeline. In this case, several zones of contact interaction were considered.

In the contact zones, which mainly affect the transfer of forces between the interacting elements, the grid thickens with a decrease in the size of the finite element to 1 mm. When modeling contact interaction, an eight-unit contact finite element was used to describe contact and sliding between surfaces (Fig. 3).

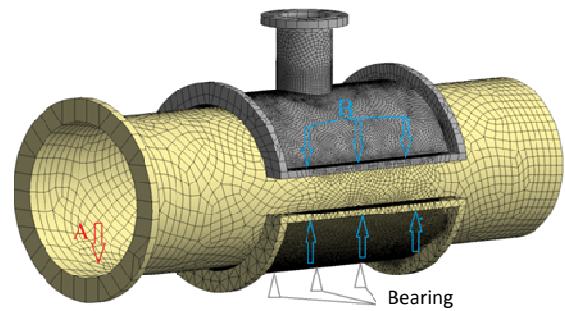


Fig. 1. Computational model of the connecting unit of the turbine steam line

Table 1. Physical and mechanical properties of sealing unit materials

Material	Physical and mechanical properties		
	$E \cdot 10^{-3}$, MPa	ν	ρ , kg/m ³
Steal 15CrMoV5-10 (pipeline, casing)	217	0.3	7,800
Paronite FA-MN13-O (gasket seal)	1.2	0.3	2,000

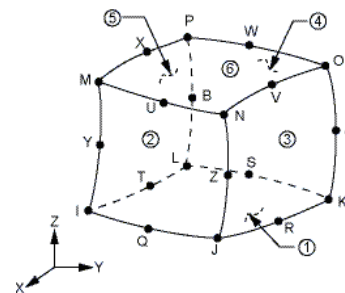


Fig. 2. Geometry of twenty-unit FE

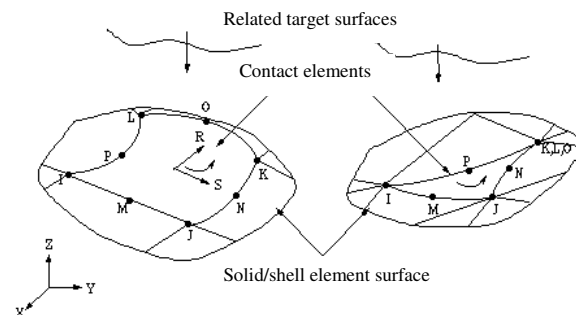


Fig. 3. Geometry of the eight-unit contact FE

According to [6], the boundary contact problem is characterized by the presence of a contact zone of a known (stable) or unknown (unstable, variable) configuration. In this zone, there is no interpenetration of the surfaces of bodies, and the forces transferred as a result of contact cannot be tensile (taking into account the forces of surface adhesion in the contact zone, a certain level of "negative pressure" is allowed). According to the consequence of the general conservation law (the law of surface interactions), the contact forces on two contact surfaces must be equal in magnitude and multidirectional. In this case, the force contact can be carried out both with friction and without friction. As a result, the formulation of the boundary contact problem includes additional contact conditions and constraints, which can be described by the following equations, on the contact surface S_k .

On the general surface S_k of elements with conditional numbers 1 and 2, the following coupling conditions must be satisfied:

– force for stresses σ

$$(\sigma_{(1)}^{mn} - \sigma_{(2)}^{mn}) \cdot \mathbf{v}_{m(j)} = 0, \quad m, n = 1, 2, 3, \quad j = 1, 2; \quad (1)$$

– kinematic during adhesion (displacement of U in the same basis as the coordinates x)

$$[(x_m + U_m)_{(1)} - (x_m + U_m)_{(2)}] \cdot \mathbf{v}_m = 0, \quad m = 1, 2, 3, \quad (2)$$

$$[(x_m + U_m)_{(1)} - (x_m + U_m)_{(2)}] \cdot \boldsymbol{\tau}_m = 0, \quad m = 1, 2, 3, \quad (3)$$

where \mathbf{v}_m , $\boldsymbol{\tau}_m$ respectively, vectors components of the outer normal to contact surface and tangent to this surface. During slipping (with or without friction), condition (3) is not used.

Among the set conditions are:

– negative values of normal components of contact forces

$$(\sigma^{mn} \mathbf{v}_m \mathbf{v}_n)_{(j)} < 0, \quad j = 1, 2; \quad (4)$$

– mutual non-penetration of bodies

$$[(x_m + U_m)_{(1)} - (x_m + U_m)_{(2)}] \cdot \mathbf{v}_m \leq 0. \quad (5)$$

Inequalities (4), (5) are the basis for the determination of the current contact surface configuration.

The force interaction of surfaces in the contact zone S_k can occur under conditions of adhesion or slippage.

In the case of adhesion, that is, with $|\sigma_\tau| \leq \min\{\mu|\sigma_v|, (\sigma_s)_{\min} / \sqrt{3}\}$ (σ_s is actual material yield strength),

$$\sigma_v = \sigma^{mn} \mathbf{v}_m \mathbf{v}_n \Big|_{S_k} = \widehat{F}_v, \quad (6)$$

$$\sigma_\tau = \left[\sum_{n=1}^3 (\sigma^{mn} \mathbf{v}_m)^2 - (\sigma^{mn} \mathbf{v}_m \mathbf{v}_n)^2 \right]^{1/2} \Big|_{S_k} = \widehat{F}_\tau \quad (7)$$

or

$$U_m \Big|_{S_k} = \widehat{U}_m. \quad (8)$$

During slipping, that is, when $|\sigma_\tau| > \min\{\mu|\sigma_v|, (\sigma_s)_{\min} / \sqrt{3}\}$ we have

$$\sigma_v = \sigma^{mn} \mathbf{v}_m \mathbf{v}_n \Big|_{S_k} = \widehat{F}_v \quad (9)$$

or

$$U_v = U_m \mathbf{v}_m \Big|_{S_k} = \widehat{U}_v, \quad (10)$$

and also, at $\mu \neq 0$

$$\sigma_\tau = -|\widehat{F}_\tau| \cdot \text{sign}(U_\tau), \quad (11)$$

where $U_\tau = (U_{m(1)} - U_{m(2)}) \cdot \boldsymbol{\tau}_m$ is projection of the vector of mutual displacements, tangent to the contact surface.

If there is no need to take friction into account (if the coefficient of friction μ is equal to zero) during the calculation, then these conditions are simplified to

$$\sigma_v = \sigma^{mm} \mathbf{v}_m \mathbf{v}_n \Big|_{Sk} = \widehat{F}_v \text{ or } U_v = U_m \mathbf{v}_m \Big|_{Sk} = \widehat{U}_v. \quad (12)$$

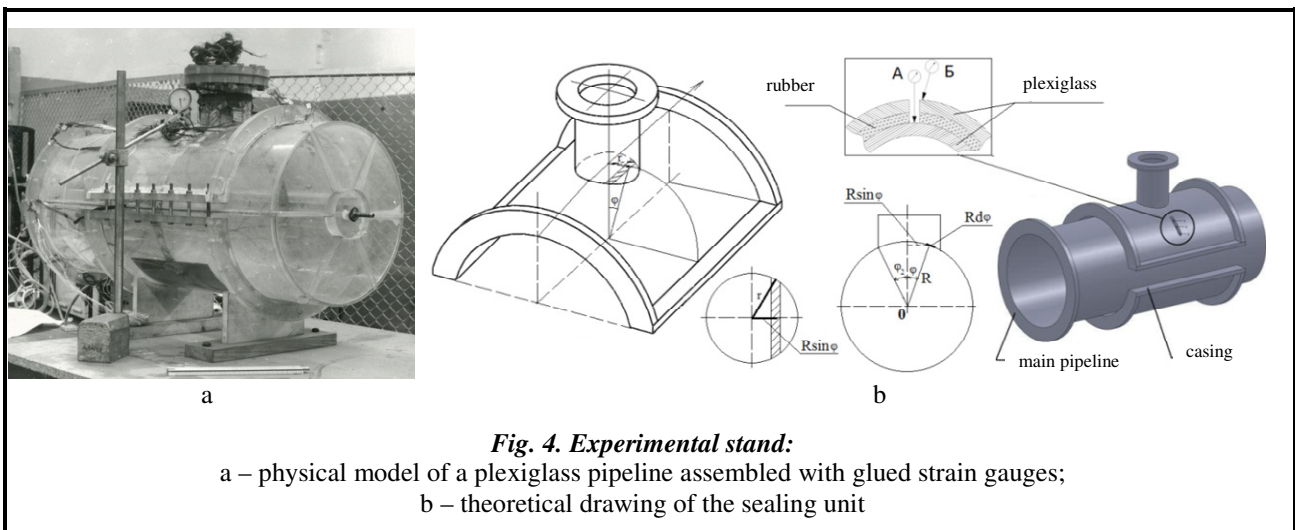
Solution method

In the process of minimizing the target FEM functional, additional constraints (1)–(12) are usually taken into account by one of two methods: penalty method (PM) and Lagrange multiplier (LM). PM is distinguished by its economy of memory and time resources and has become quite widespread when solving frictional contact problems. In turn, LM is known for its accuracy [7]. However, it may lead to incorrect convergence of the solution.

Taking into account the need to quickly solve contact problems that arise during the production and operation of power equipment, the PM was adopted to solve the considered problem. In contact problems, the penalty term includes the stiffness matrix of the contact surface. This matrix stems from the concept that one imaginary body penetrates into another [8].

Model experiment

To verify the proposed model and solution technique, an experimental study of the stress-strain state was carried out with the use of strain gauging [10] of the pipeline unit on a physical model made of a low-modulus material – plexiglass [11] at a scale of 1:2.5 with full geometric similarity (Fig. 4). As primary transducers, paper-based strain gauges with a 5 mm base were used. The scheme of the strain gauges location was taken according to [12].



The physical model of the pipeline is a cylindrical pipe 400 mm in diameter and 4 mm thick. Flat plexiglass sheets served as billets. After heating in the furnace, the billets were crimped on a specially made cylindrical mandrel, and took the required shape. A cylindrical tube was formed from the obtained elements. Plugs were installed from the ends. One of the plugs was welded, and the second one, removable, was bolted to the flange. The removable plug has a special device for the wires removal from the sensors located on the inner surface.

As seen from Fig. 4, the main pipe is covered by a casing with a branch, which is also made of plexiglass. The casing consists of two halves for which there are horizontal joint flanges. For rigidity, annular flanges are welded on the ends of the casing. The two halves of the casing were pulled together with metal studs. The space between the casing and the main pipeline was filled with thick soft sheet rubber, which contributes to a more uniform transfer of force to the surface of the main pipeline during crimping by the casing. The stiffness (elastic modulus) ratio of plexiglass and rubber is the same as in a full-scale structure.

The stresses were measured mainly in the circumferential section at a plane passing through the center of the hole perpendicular to the pipe axis, i.e., in the direction along which the contact pressure was measured. Since the stresses were measured along the direction of the main curvatures of the pipe (in

circumferential and axial directions), it would be enough to use double sockets. Nevertheless, to determine possible misalignments during loading, sensors were also installed along the bisector of the angles between the axial and circumferential directions. Considering possible unevenness of stress distribution in the hole area, the sensors were installed as often as possible [9, 13]. To do this, we had to abandon the location of strain gauges in the form of traditional triple sockets and use the so-called "chain" scheme, which consists of three groups of sensors. The sensors of the first group are oriented in the axial direction, the second group – in the circumferential direction, and the third group – at an angle of 45° to the first two directions. Although the directions of the sensors of the first and second groups coincide with the directions of the main curvatures and, due to symmetries, one would expect them to coincide with the directions of main stresses, sensors of the 3rd group were used to fix possible distortions.

The test procedure was carried out as follows. The pressure, which was transmitted through the rubber gasket from the casing seal, was created on the pipe surface. It was created by the tightening force of the studs tightening the flanges of the horizontal joint of the casing. Due to the fact that the forces transmitted by the casing to the pipe, hereinafter referred to as contact pressure, are uneven along the pipe surface, it became necessary to measure the pressures at several points. For this, a narrow slot in the annular direction was cut in the tee casing and in the rubber layer, which made it possible to position both indicators from the outer surface: the needle of one rested against the pipe, the needle of the other – against the tee casing [9]. Thus, by the change in the thickness of the rubber gasket, one can estimate the contact pressure value. The measurements were carried out according to the scheme shown in Fig. 4. The value of rubber compression was determined as the difference between displacements measured by indicators A and B. For the transition from the value of rubber compression to the value of the contact pressure, calibration has been carried out. For this, a rubber sample $20\text{ mm} \times 20\text{ mm} \times 8\text{ mm}$ was subjected to uniform crimping. The rubber gasket deformation (thickness reduction) was measured depending on the applied force.

The thickness of the casing - gasket - pipe system was found from the expression

$$\delta = (m_u^1 - m_u^0) + (m_l^1 - m_l^0),$$

where m – the coordinate of the sensor needle, the subscripts "u" and "l" mean the upper and lower sensors respectively, the superscripts 1 and 0, respectively, the moment after and before crimping.

Since the elastic modulus of rubber is several thousand times less than the one of plexiglass, we believe that the change in the gap occurred only due to the compression of the rubber.

Deformation measurements of the rubber gasket were carried out for various crimping forces of the seal. Fig. 5 shows the experimental points and the curve that approximates them. Based on the obtained results, compression calibration was carried out with the determination of the rubber seal thickness dependence on the applied load. Thus, using the dependence shown in Fig. 5, it is possible to find the value of the contact pressure in the system, as well as the dependence between the applied force and contact pressure

$$P_2 = \int_{-\varphi_2}^{+\varphi_2} \int_{-\sqrt{r^2 - R^2 \sin^2 \varphi}}^{\sqrt{r^2 - R^2 \sin^2 \varphi}} q_0 \cos \varphi \cos \varphi dF = \int_{-\varphi_2}^{+\varphi_2} q_0 \cos^2 \varphi R d\varphi \int_{-\sqrt{r^2 - R^2 \sin^2 \varphi}}^{\sqrt{r^2 - R^2 \sin^2 \varphi}} dx = 2q_0 R \int_{-\varphi_2}^{+\varphi_2} \sqrt{r^2 - R^2 \sin^2 \varphi} \cos^2 \varphi d\varphi,$$

where P_2 is the value of force that would act on the gasket, which has the shape of a circle of radius r , the center of which lies in the vertical plane of symmetry; q_0 is the amplitude value of the contact pressure (in the plane perpendicular to the connector), kg/cm^2 ; R is the radius of the middle surface of the shell, cm; r is the hole radius, cm; φ_2 is the angle shown in Fig. 4, b, can be easily found on the basis of the geometric dimensions of the considered pipeline element.

Along with the contact pressure, stresses were also measured. In order to separate bending and tensile stresses, strain gauges were glued to inner and outer surfaces. At the same time, a strict match was observed: each sensor on one surface has a corresponding sensor on the other. Due to the fact that the shells under study are essentially thin-walled (the ratio of the wall thickness to the radius of curvature is $\frac{0.4\text{ cm}}{6\text{ cm}} = \frac{1}{15}$ in main pipeline and $\frac{0.4\text{ cm}}{20\text{ cm}} = \frac{1}{50}$ in the branch), with a high degree of accuracy, the law of stress variation across the wall thickness can be considered linear. Hence it follows that bending stresses

$\sigma_b = \frac{\sigma_{int} - \sigma_{ext}}{2}$ and tensile (membrane) stresses are determined by the formula $\sigma_t = \frac{\sigma_{int} + \sigma_{ext}}{2}$, where σ_{ext} and σ_{int} are the stress on the external and internal surface of some direction, respectively.

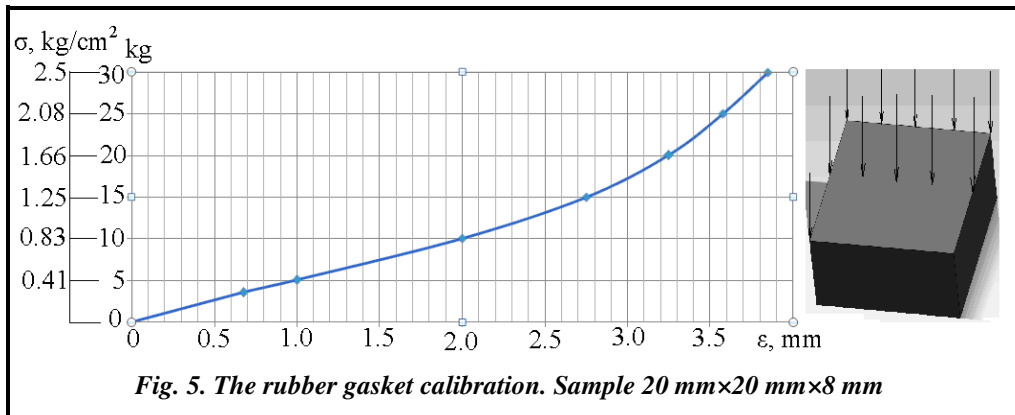


Fig. 5. The rubber gasket calibration. Sample 20 mm x 20 mm x 8 mm

Verification of the calculation model and software

To prove the adequacy of the proposed model, the methodology for solving the considered contact problem and the software that implements the proposed approach, the obtained experimental results were compared with the results of calculation performed with the initial data corresponding to the physical model described above. The physical and mechanical properties of the materials of the physical model are presented in table 2.

Table 2. Physical and mechanical properties of the pipeline sealing unit materials

Material	Physical and mechanical properties		
	E, MPa	v	ρ, kg/m³
Organic glass (pipeline, casing)	2.785 × 10³	0.35	1190
Soft porous rubber (seal)	1	0.30	1800

Just as in the tests on the physical model, the stress-strain state of a pipeline element was simulated under loading by pressure created by the tightening force of the studs – 0.016 MPa, and by internal pressure on the steam line wall, that is 0.02 MPa. The general diagram of the application of the boundary conditions is shown in Fig. 1.

Comparison of the results of the physical experiment and the model calculation of the pipeline sealing unit showed that the deflection values (absolute deformation of the rubber gasket in the direction of pressure from the casing seal, Fig. 6, a) and contact pressures on the contacting surface of the pipeline under the upper half of the casing (Fig. 6, b), as well as the values of axial and circumferential tensile and bending stresses, have a very good agreement in the investigated sections.

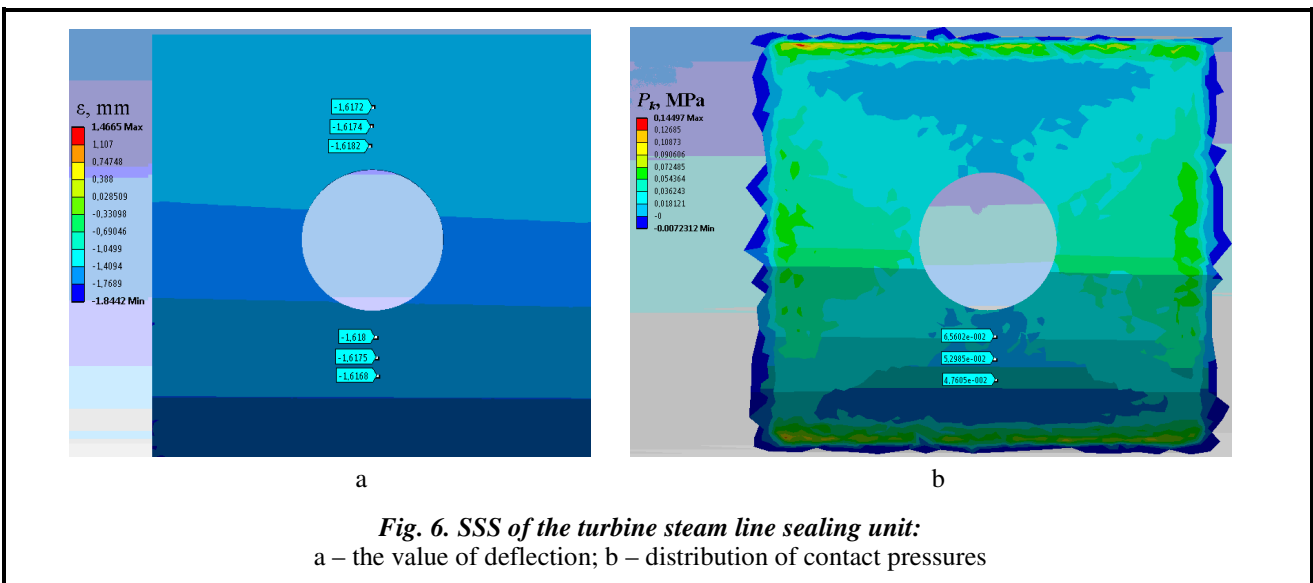


Fig. 6. SSS of the turbine steam line sealing unit: a – the value of deflection; b – distribution of contact pressures

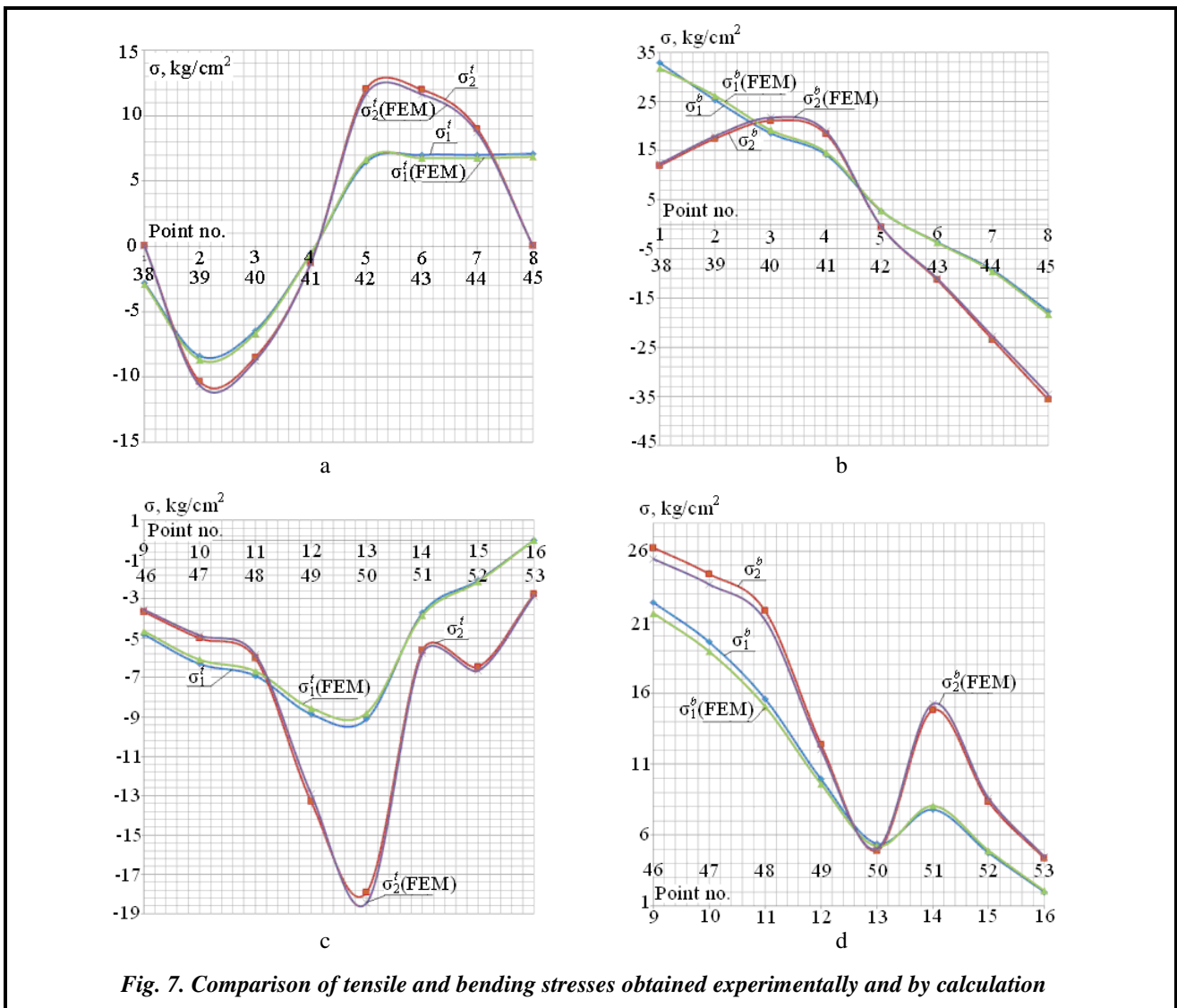
Table 3 shows the values of contact pressures at the points of installation of indicators on the surface of the main pipeline and the deflections of the seal under the action of the load created by the studs tightening [14]. It is seen from the table that the difference between the calculated and experimental data does not exceed 6% for contact pressures and 12% for deformations.

Table 3. Summary results of the contact problem study

Measuring point no.	Deflection, mm		Contact pressure, MPa	
	Experiment	Calculation	Experiment	Calculation
1, 4	1.43	1.6180	0.062	0.0656
2, 5	1.38	1.6175	0.050	0.0530
3, 6	1.44	1.6168	0.045	0.0476

Based on the obtained results, stress curves presented in Fig. 7 were plotted, where $\sigma_1^t, \sigma_2^t, \sigma_1^b, \sigma_2^b$ are respectively, axial and circumferential stretching and bending stresses obtained experimentally; $\sigma_1^t(\text{FEM}), \sigma_2^t(\text{FEM}), \sigma_1^b(\text{FEM}), \sigma_2^b(\text{FEM})$ are respectively, axial and circumferential tensile and bending stresses obtained by calculation.

These stresses are given at the points of installation of strain gauges on the inner (Fig. 7, a and 7, b) and outer surfaces of the pipeline (Fig. 7, c and 7, d) in the area of the hole, that is, under the casing seal. In this area, the sensors were installed as often as possible, due to the uneven distribution of stresses.



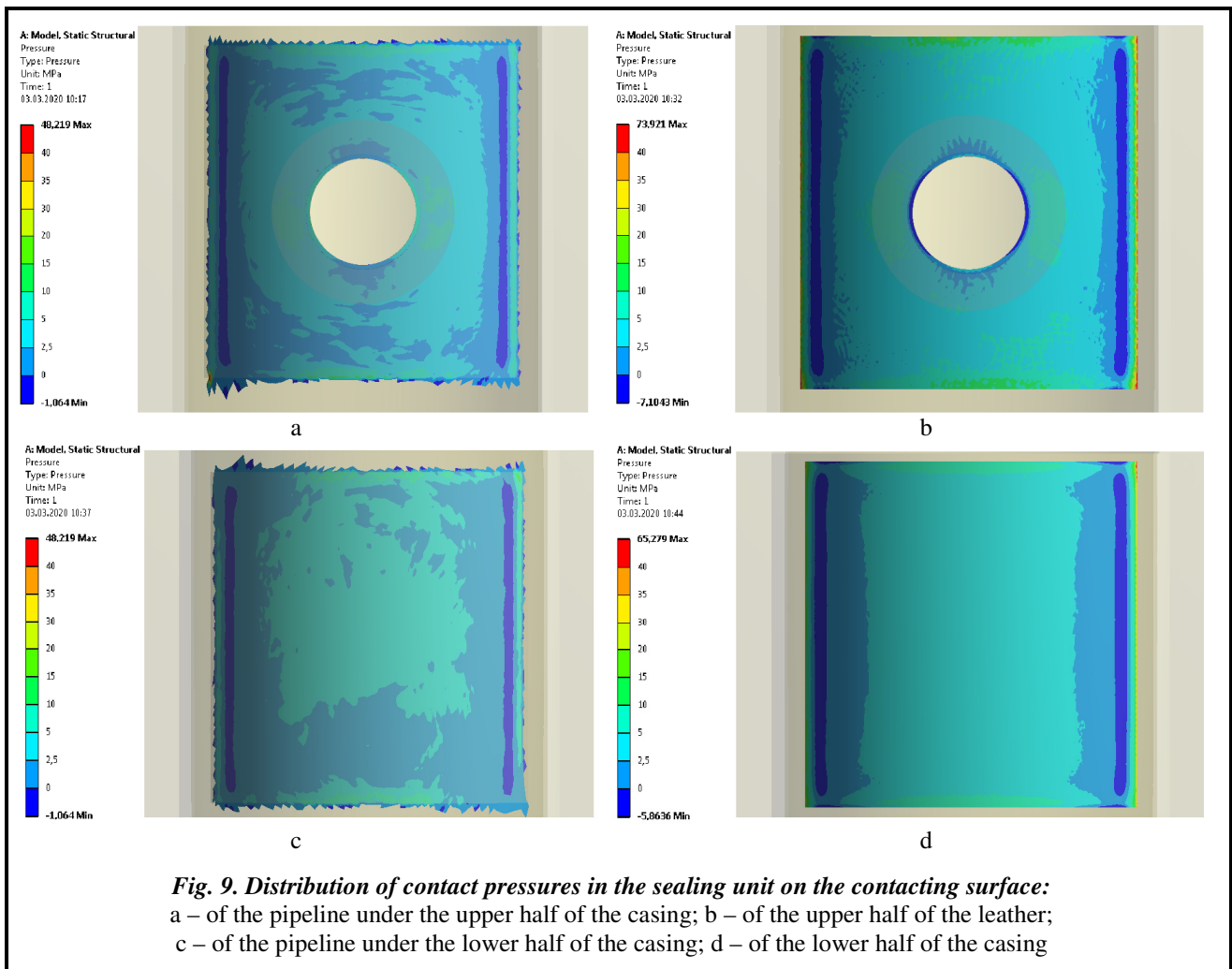
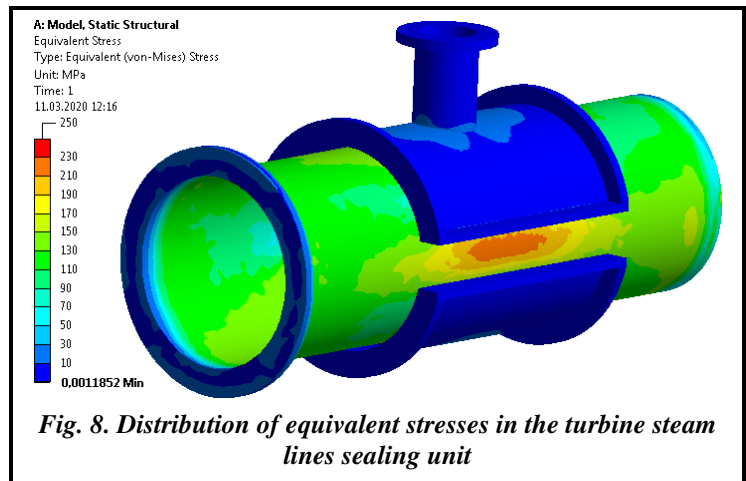
Analysis of calculation results

Verified software for solving the contact problem of the pipeline unit deformation was used to determine the stress-strain state of the real pipeline unit. Fig. 8 shows the nature of the stress distribution, and Fig. 9 – contact pressure on the surface of the pipeline under the seal under the influence of the tightening force of the studs.

The calculation results showed that the maximum local stresses are observed on the surface of the pipeline, between the upper and lower halves of the casing, and are about 250 MPa (see Fig. 8), which is associated with material deformation from high contact pressure

on the sealing surface. In the area of the main steam line flange, a surge of stresses is observed only in the welding zone and is about 60 MPa, on average, the stresses in the area of the body flanges are insignificant – less than 30 MPa, which is fully complies with the regulatory requirements [9]. In the sealing unit, namely, in the section where the pipe is welded to the casing, the stresses averaged over the wall thickness are about 50 MPa.

Fig. 9 shows the distribution of the contact pressure transmitted from the casing seal through the rubber seal to the surface of the main pipeline under the action of the load created by the studs tightening.



Based on the obtained results, it can be concluded that there are areas with a significant local increase in the stresses of the pipeline body in the sealing unit, as well as zones with a negative level of contact pressure on the contacting surfaces. This circumstance must be taken into account during the pipelines designing and operation. Thus, the proposed methodology and the developed software will be in demand when solving such problems.

Conclusions

A mathematical model has been compiled and a methodology for solving the contact problem of the pipeline sealing unit has been developed. This technique is based on the use of FEM in conjunction with the penalty method, in which the penalty is organized according to the conditions of the contact.

In order to verify the proposed approach and software that implements this technique, an experimental and numerical study of the stress-strain state of the model pipeline sealing unit made of a low-modulus material and representing a test model was carried out. The results obtained on the physical model by the strain gauge method and with the calculation according to the proposed method showed pretty good agreement (up to 7–10%).

The stress-strain state of the real pipeline sealing unit in a three-dimensional setting was determined, and the most stressed zones in the unit that require increased attention during the design and operation of pipelines and their sealings were identified. The following things were established:

- the stress state of the sealing unit is three-dimensional and a complex deformation pattern is observed;
- in general, the level of stresses in the unit walls is low, but there are zones of increased stress on the surface of the pipeline, between the upper and lower halves of the casing;
- the distribution of the contact pressure transmitted from the casing seal through the rubber seal to the surface of the main pipeline under the action of the load created by the studs tightening showed the presence of areas with a negative level of contact pressure on the contacting surfaces.

Application of the developed computational approach makes it possible to determine the contact pressure for the horizontal joint flanges of high-stress cylinder bodies of powerful steam turbines. In most cases, the experimental data on such connectors are absent due to many factors, such as the complexity of the model manufacturing and the large material costs to conduct multivariate experiments for various geometry options. Therefore, the proposed methodology and the developed software will be in demand when solving such problems.

-References

1. Kalyutik, A. A. & Sergeev, V. V. (2003). *Truboprovody teplovykh elektricheskikh stantsiy* [Pipelines of thermal power plants]: A tutorial. St. Petersburg: Publishing House of St. Petersburg Polytechnic University, 50 p. (in Russian).
2. Prigorovskiy, N. I. & Preys, A. K. (1958). *Issledovaniye napryazheniy i zhestkosti detaley mashin na tenzometricheskikh modelyakh* [Study of stresses and stiffness of machine parts on tensometric models]. Moscow: AN SSSR, 232 p. (in Russian).
3. (2011). *Issledovaniye vliyaniya konstruktivnykh razmerov kozhukha-troynika na napryazhenno-deformirovannoye sostoyaniye uzla uplotneniya osnovnogo gazoprovoda* [Study of the influence of the design dimensions of the tee casing on the stress-strain state of the seal assembly of the main gas pipeline]: Report on research work No. D-4089; Research Director – Kabanov, A. F. Kharkov: Special Design Bureau "Turboatom", 96 p. (in Russian).
4. (Turenko, A. N., Bogomolov, V. A., Stepchenko, A. S., Kedrovskaya, O. V., & Klimentko, V. I. (2003). *Kompyuternoye proyektirovaniye i raschet na prochnost detaley avtomobilya* [Computer design and strength calculation of car parts]: A tutorial. Kharkiv: Kharkiv Highway University, 336 p. (in Russian).
5. Deryagin, A. A. (2013). *Formoobrazovaniye i animatsiya 3D-obyektov na osnove tetragonalnoy regulyarnoy setki* [Shaping and animation of 3D objects based on a tetragonal regular grid]. *Prikladnaya informatika – Journal of Applied Informatics*, no. 2 (44), pp. 94–101 (in Russian).
6. Tolok, V. A., Kirichevskiy, V. V., Gomenyuk, S. I., Grebenyuk, S. N., & Buvaylo, D. P. (2003). *Metod konechnykh elementov. Teoriya, algoritmy, realizatsiya* [Method of finite elements. Theory, algorithms, implementation]. Kiev: Naukova Dumka, 283 p. (in Russian).
7. Stefanu, A. I., Melenciuc, S. C., & Budescu, M. (2011). Penalty based algorithms for frictional contact problems. *The Bulletin of the Polytechnic Institute of Jassy*. Section: Architecture. Construction, no. 3, pp. 54–58.
8. Wriggers, P., Vu Van, T., & Stein, E. (1990). Finite element formulation of large deformation impact-contact problems with friction. *Computers & Structures*, vol. 37, iss. 3, pp. 319–331. [https://doi.org/10.1016/0045-7949\(90\)90324-U](https://doi.org/10.1016/0045-7949(90)90324-U).

9. Guz, A. N., Chernyshenko, I. S., Chekhov, V. N., Chekhov, V. N., & Shnerenko, K. I. (1974). *Tsilindricheskiye obolochki, oslablennyye otverstiyami* [Cylindrical shells weakened by holes]. Kiyev: Naukova Dumka, 272 p. (in Russian).
10. Perlin, A. A., Shalkin, M. K., & Khryashchev, Yu. K. (1967). *Issledovaniye prochnosti sudovykh konstruksiy na tenzometricheskikh modelyakh* [Research of the strength of ship structures on tensometric models]. Leningrad: Sudostroyeniye, 80 p. (in Russian).
11. Gudimov, M. M. & Perov, B. V. (1981). *Organicheskoye steklo* [Organic glass]. Moscow: Khimiya, 216 p. (in Russian).
12. (2013). *Usovershenstvovaniye i vnedreniye sposoba opredeleniya kontaktnogo davleniya v uzle uplotneniya osnovnogo gazoprovoda po rezultatsam tenzometrirovaniya* [Improvement and implementation of a method for determining the contact pressure in the seal unit of the main gas pipeline based on the results of strain gauging]: Report on research work No. D-4473; Research Director – Kabanov, A. F. Kharkov: Special Design Bureau "Turboatom", 50 p. (in Russian).
13. Savin, G. N. (1968). *Raspredeleniye napryazheniy okolo otverstiy* [Distribution of stresses around the holes]. Kiyev: Naukova Dumka, 891 p. (in Russian).
14. Prigorovskiy, N. I. (1982). *Metody i sredstva opredeleniya poley deformatsiy i napryazheniy* [Methods and means for determining the fields of deformations and stresses]. Moscow: Mashinostroyeniye, 248 p. (in Russian).

Received 28 August 2020

Контактне деформування вузла ущільнення трубопроводу

¹ А. О. Костіков, ² С. А. Пальков

¹ Інститут проблем машинобудування ім. А. М. Підгорного НАН України,
61046, Україна, м. Харків, вул. Пожарського, 2/10

² Акціонерне товариство «Турбоатом», 61037, Україна, м. Харків, пр. Московський, 199

Досліджено особливості напружено-деформованого стану сполучного вузла паропроводу турбоустановки на основі використання тривимірної розрахункової моделі конструкції і поверхонь, що контактують між собою. Вузол, що розглядається, включає в себе власне трубопровід, обжимний кожух, що складається з двох половин, в одній з яких встановлено відведення, і прокладку-ущільнювач. Сформовано математичну модель, що враховує механічні навантаження, які викликані як внутрішнім тиском пари на стінку паропроводу, так і затягуванням кріплень кожуха. Розглянута модель також включає контактну взаємодію в вузлі ущільнення на контактних поверхнях трубопроводу, верхньої та нижньої половин кожуха. Запропоновано методику розв'язання даної контактної задачі, яка ґрунтується на використанні методу скінченних елементів. В основу скінченноелементної моделі покладено двадцативузлові тривимірні скінченні елементи з трьома ступенями свободи в кожному вузлі. Для опису контакту і ковзання між поверхнями використовувалися восьмиузлові контактні скінченні елементи. Врахування контактних умов здійснювалося за допомогою методу штрафних функцій. Проведено верифікацію моделі і програмного забезпечення, що реалізує запропоновану методику, шляхом порівняння результатів розрахунку і експериментальних даних, які отримані на фізичній моделі трубопроводу. Фізична модель була виготовлена з низькомодульного матеріалу з дотриманням повної геометричної подібності і такого ж співвідношення модулів пружності матеріалів, як і в реальному об'єкті. Визначено напружено-деформований стан сполучного вузла реального трубопроводу в тривимірній постановці і виявлено найбільш напружені зони в вузлі, що потребують підвищеної уваги під час проектування та експлуатації трубопроводів та їх з'єднань. Розроблений підхід і програмне забезпечення дають можливість визначити контактний тиск для фланців горизонтального роз'єму високонапружених корпусів циліндрів потужних парових турбін, що дозволяє уникнути великої кількості дорогих експериментальних досліджень.

Ключові слова: турбоустановка, трубопровід, фланцеве з'єднання, контактна задача, напружено-деформований стан, контактний тиск.

Література

1. Калютік А. А., Сергеев В. В. Трубопроводы тепловых электрических станций: учеб. пособие. СПб.: Изд-во СПб политехн. ун-та, 2003. 50 с.
2. Пригоровский Н. И., Прейсс А. К. Исследование напряжений и жесткости деталей машин на тензометрических моделях. М.: АН СССР, 1958. 232 с.

3. Исследование влияния конструктивных размеров кожуха-тройника на напряженно-деформированное состояние узла уплотнения основного газопровода: отчет о НИР/ СКБ «Турбоатом». Рук. Кабанов А. Ф.; Инв. № Д-4089. Харьков, 2011. 96 с.
4. Туренко А. Н., Богомолов В. А., Степченко А. С., Кедровская О. В., Клименко В. И. Компьютерное проектирование и расчет на прочность деталей автомобиля: учеб. пособие. Харьков: Харьк. автодор. ун-т, 2003. 336 с.
5. Дерягин А. А. Формообразование и анимация 3D-объектов на основе тетрагональной регулярной сетки. *Прикл. информатика*. 2013. № 2 (44). С. 94–101.
6. Толок В. А., Киричевский В. В., Гоменюк С. И., Гребенюк С. Н., Бувайло Д. П. Метод конечных элементов. Теория, алгоритмы, реализация. Киев: Наук. думка, 2003. 283 с.
7. Stefanu A. I., Melenciuc S. C., Budescu M. Penalty based algorithms for frictional contact problems. *The Bulletin of the Polytechnic Institute of Jassy*. Section: Architecture. Construction. 2011. No. 3. P. 54–58.
8. Wriggers P., Vu Van T., Stein E., Finite element formulation of large deformation impact-contact problems with friction. *Computers & Structures*. 1990. Vol. 37. Iss. 3. P. 319–331. [https://doi.org/10.1016/0045-7949\(90\)90324-U](https://doi.org/10.1016/0045-7949(90)90324-U).
9. Гузь А. Н., Чернышенко И. С., Чехов В. Н., Чехов В. Н., Шнеренко К. И. Цилиндрические оболочки, ослабленные отверстиями. Киев: Наук. думка, 1974. 272 с.
10. Перлин А. А., Шалкин М. К., Хрящев Ю. К. Исследование прочности судовых конструкций на тензометрических моделях. Л.: Судостроение, 1967. 80 с.
11. Гудимов М. М., Перов Б. В. Органическое стекло. М: Химия, 1981. 216 с.
12. Усовершенствование и внедрение способа определения контактного давления в узле уплотнения основного газопровода по результатам тензометрирования: отчет о НИР/ СКБ «Турбоатом». Рук. Кабанов А. Ф.; Инв. № Д-4473. Харьков, 2013. 50 с.
13. Савин Г. Н. Распределение напряжений около отверстий. Киев: Наук. думка, 1968. 891 с.
14. Пригоровский Н. И. Методы и средства определения полей деформаций и напряжений. М.: Машиностроение, 1982. 248 с.